Biochimica et Biophysica Acta 806 (1985) 81–92
Elsevier

BBA 41676

Chlorophyll fluorescence phenomena in chloroplasts on subnanosecond time-scales probed by picosecond pulse pairs †

A. Dobek [a,*], J. Deprez [a], N.E. Geacintov [b], G. Paillotin [a] and J. Breton [a]

[a] *Service de Biophysique, Département de Biologie, Centre d'Etudes Nucléaires de Saclay, 91191 Gif-sur-Yvette Cedex, (France) and* [b] *Chemistry Department, New York University, New York, NY 10003 (U.S.A.)*

(Received May 16th, 1984)
(Revised manuscript received September 19th, 1984)

Key words: Fluorescence induction; Chlorophyll fluorescence; Photosystem II; Exciton; Reaction center; (Spinach chloroplast)

Fluorescence enhancement phenomena and quenching by exciton-exciton annihilation on subnanosecond and nanosecond time-scales were investigated in spinach chloroplasts utilizing picosecond laser pulse pairs (530 nm, 30 ps wide) of equal intensity, spaced apart in time by variable delays of $\Delta t = 0$–6 ns. This new method was devised to study the effect of pulse energies ($1 \cdot 10^{10}$–$2 \cdot 10^{15}$ photons per cm^2) on the overall fluorescence yield in order to deduce the degree of correlation between the two pulses as a function of Δt. In the case of open reaction centers (F_0 state) in Photosystem II (PS II), it is shown that the quenching effect of excitons generated by the first pulse on the fluorescence yield of the second pulse diminishes with increasing Δt with a characteristic decorrelation time of 140 ± 60 ps. This effect is attributed to either (1) the decay of mobile excitons in the light-harvesting antenna pigment bed as these excitons migrate towards the PS II reaction centers and the associated smaller core antenna pigment pools, or (2) the decay of a quenching state of the reaction center (and/or core antenna) which appears following a rapid (less than 140 ps) trapping of the excitons initially created in the antenna pigment bed. The absence of a significant decay component of exciton quenchers with a lifetime comparable to the 300–600 ps intermediate phase of fluorescence decay kinetics suggests that this phase, although contributing to more than half of the integrated fluorescence emission signal, is not caused by freely mobile exitons migrating in a lake of pigments, but originates instead from smaller pigment pools to which the excitons have migrated. It is proposed that bimolecular exciton-exciton annihilation in these smaller domains dominates annihilation in the larger antenna pigment bed. In the case of closed reaction centers (F_{max} state), the decorrelation time between the two pulses is increased to 400 ± 100 ps, which is also attributed to either a mobile exciton component or to the decay of a quenching state of the reaction center. At low pulse intensities (below approx. $2 \cdot 10^{12}$ photons per cm^2) anomalous fluorescence enhancement effects are noted, which are clearly linked to the existence of initially open PS II reaction centers. These enhancement effects are different from the well-known fluorescence induction phenomena which occur on longer time-scales, and are tentatively attributed to variations in the quenching efficiencies of transitory photochemical states of PS II reaction centers.

† This paper is dedicated to the memory of Professor Warren L. Butler.

* On leave from the Quantum Electronics Laboratory, Institute of Physics, A. Mickiewicz University, Poznan, Poland.

Abbreviations: PS II, Photosystem II; P-680, primary donor; I, intermediate acceptor; Q, first quinone acceptor.

Introduction

In steady-state illumination experiments, the fluorescence yield of chloroplasts isolated from green plants is about 3–5-times higher [1] when

the PS II reaction centers are all closed (F_{max}) than when they are open (F_0). The time required to reach the F_{max} level depends on the light intensity [2], and is generally of the order of milliseconds or seconds, depending on the intensity of the steady-state illumination. Utilizing high-intensity laser pulses, even as short as nanoseconds [3] or picoseconds [4] in duration, it is possible to close most or all of the reaction centers. Double-pulse techniques have been used to probe the kinetics of the fluorescence induction phenomenon; utilizing a nanosecond duration actinic laser pulse, Mauzerall [3,5] found that the risetime of the fluorescence is 60 ns. Our recent experiments [4] utilizing pairs of picosecond laser pulses indicate that the first-order time constant for this rise is 28 ± 4 ns. As described by Butler [6] both the open (P-680) and oxidized (P^+-680) reaction centers are fluorescence quenchers. Therefore, this fluorescence induction phase is attributed to the reduction of P^+-680 in Photosystem II reaction centers by a primary donor. However, there are indications that the behavior of the fluorescence yield on timescales of 1 ns or shorter is more complex than indicated by these simple considerations. Utilizing single, 8 ± 1 ps wide (530 nm) picosecond laser pulses of varying energies, Hirsh et al. [7] noted that the fluorescence yield of dark-adapted *Zea mays* L. leaves increased by about 30% as the pulse energy was increased from 10^{12} to 10^{14} photons per cm^2. At still higher energies, the usual decrease in the yield, attributed to exciton-exciton annihilation [8–10], was observed. We have obtained similar results utilizing dark-adapted spinach chloroplasts and somewhat wider pulses (30 ps) at the same excitation wavelength [4]. Sonneveld et al. [11] also observed a rise in the fluorescence yield with *Chlorella vulgaris* using much longer, 15 and 30 ns, pulses. While in the case of Sonneveld et al. this increase in the integrated fluorescence yield at low pulse energies can be attributed to the reduction of P^+-680, the origin of this increased yield must be quite different in the single picosecond laser pulse experiments [4,7].

Another complicating feature in such experiments is the known heterogeneity of the fluorescence. Recent low-energy laser excitation single-photon counting techniques have established that the fluorescence decay profiles are multiphasic and are best represented by a sum of three exponential decays. With dark-adapted chloroplasts or algae (open reaction centers), two fluorescence decay components with lifetimes of 100–130 ps and 400–500 ps are dominant. When the reaction centers are closed, a third component with a lifetime of 1–2 ns becomes prominent [12–15]. Since the different decay components observed by low-intensity excitation single-photon counting methods may originate from different pigment systems in photosynthetic membranes, it is of interest to determine which of the lifetime components is most strongly affected by singlet exciton-exciton annihilation. The bimolecular exciton quenching effect depends on the density of excitons and on the spatial size of the domains to which the excitons are confined [9,16]. This phenomenon may thus provide further insight into the origins of the multiple fluorescence lifetimes and the topological characteristics of the fluorescence.

In order to study these problems we have devised a special double-pulse picosecond laser excitation technique in which the separation, Δt, between the two pulses is varied between 0 and 6 ns. This technique essentially provides information concerning the effect of excitons created during the first pulse on the fluorescence yield due to the second pulse. In this technique, a single laser pulse (P_1) of approx. 30 ps is followed by a second pulse (P_2) of equal intensity a time interval $\Delta t = 0$–6 ns later. It is shown that in this range of Δt, excitons created by P_1 and capable of quenching the fluorescence generated by P_2 decay with time constants of 140 ± 60 ps and 400 ± 100 ps in the two cases of dark-adapted and light-adapted chloroplasts, respectively.

Principles of the technique

In a previous work [4] a similar double-pulse technique was utilized, but the time interval Δt was varied between 6 and 110 ns. Since in this work Δt is less than 6 ns, it was not possible to discriminate between the fluorescence signals generated by each pulse alone as in Ref. 4. Therefore a different approach was utilized.

A single 30 ps pulse was split into two components via a beam splitter, and the second pulse of nearly the same energy as the first one, was delayed by a variable time interval, Δt. The total

fluorescence measured either with pulse P_1 alone (P_2 blocked) or with both P_1 and P_2 incident on the sample were then determined. We denote the fluorescence yield (observed fluorescence signal/ incident laser pulse intensity) observed with P_1 alone by F_1, and the integrated yield observed with both pulses incident by F_{1+2}. We define the relative change in the yield as:

$$\Delta F = (F_{1+2} - F_1)/F_1 \qquad (1)$$

This quantity can be either positive, negative or zero, depending on the intensity dependence of the fluorescence yield. In Fig. 1a three different hypothetical examples of the behavior of F_1 and of F_{1+2} are shown for the case $\Delta t = 0$. It is evident that the sign of ΔF allows for a determination of whether there is an increase, or a decrease of the fluorescence yield with increasing intensity of excitation. The existence of either fluorescence induction or fluorescence quenching phenomena can thus be established by observing the sign of ΔF.

From a practical standpoint it is difficult to adjust the intensity of the pulses so that the intensities are equal, i.e., $F_1 = F_2$ (yields F_1 and F_2 are the yields obtained separately with each one of the pulses). Thus, in Eqn. 1 we have used the average value:

$$F_{12} = (F_1 + F_2)/2 \qquad (2)$$

instead of F_1 in the determination of ΔF. It is easy to show that the error in calculating ΔF is approx. 1% if there is a 20% difference in the intensities of the pulses, and only 0.2% if this difference is 10%. In our experiments, it was feasible to maintain such a small error in this approximation by maintaining the intensities of the pulses nearly constant within approx. 10%.

A typical fluorescence yield curve as a function of laser pulse intensity (single pulse) for dark-adapted chloroplasts [4,7] is shown schematically in Fig. 1b (upper curve). We note that there is a rising and a decreasing portion in the F_1 curve as the pulse intensity is increased. Clearly, the value of ΔF will depend on the interval Δt between the two pulses. If $\Delta t \to \infty$, there is no correlation between the pulses and $\Delta F = 0$. However, if $\Delta t = 0$, and the two pulses overlap in time and space, the ΔF curve exhibits complex behavior (Fig. 1b).

From the example depicted in Fig. 1, it is evident that ΔF determined for different values of Δt in the range 0–6 ns can characterize the degree of interaction between the two pulses as a function of Δt.

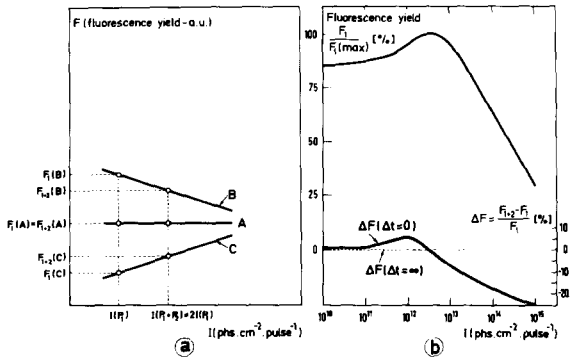

Fig. 1. (a) Schematic representation of different types of behavior of the fluorescence yield as a function of the laser pulse intensity I (for details see text). (b) Upper curve: a typical fluorescence yield curve F_1 (expressed as a percentage of the maximum) of dark-adapted chloroplasts as a function of laser intensity (single 30 ps pulse, 530 nm). Lower curve: two cases of ΔF-curves as a function of laser pulse intensity for dark-adapted chloroplasts: ΔF ($\Delta t = 0$): the two pulses overlap in time and space. $\Delta F(\Delta t = \infty)$: the two pulses are completely uncorrelated.

Experimental procedure

A complete description of the preparation of the chloroplasts, and the basic experimental apparatus have been given earlier [4]. However, this apparatus was modified in several important ways and is depicted in Fig. 2.

The laser beam was divided into two pulses P_1 and P_2, and P_1 was directed into a variable delay path ($\Delta t = 0 \to 6$ ns). The time interval betweeen the two pulses (30 ps full width at half maximum) was estimated by varying the position d of a back-reflecting mirror, and by measuring the time of arrival of the pulses at the position of the sample utilizing a fast photodiode (LR 104, Optel) and a Tektronix 7104 oscilloscope. In this manner, delays as short as 100 ps could be measured accurately; the position of the mirror for the $\Delta t = 0$ point was found by extrapolating the experimentally determined function $d = f(\Delta t)$. A set of mir-

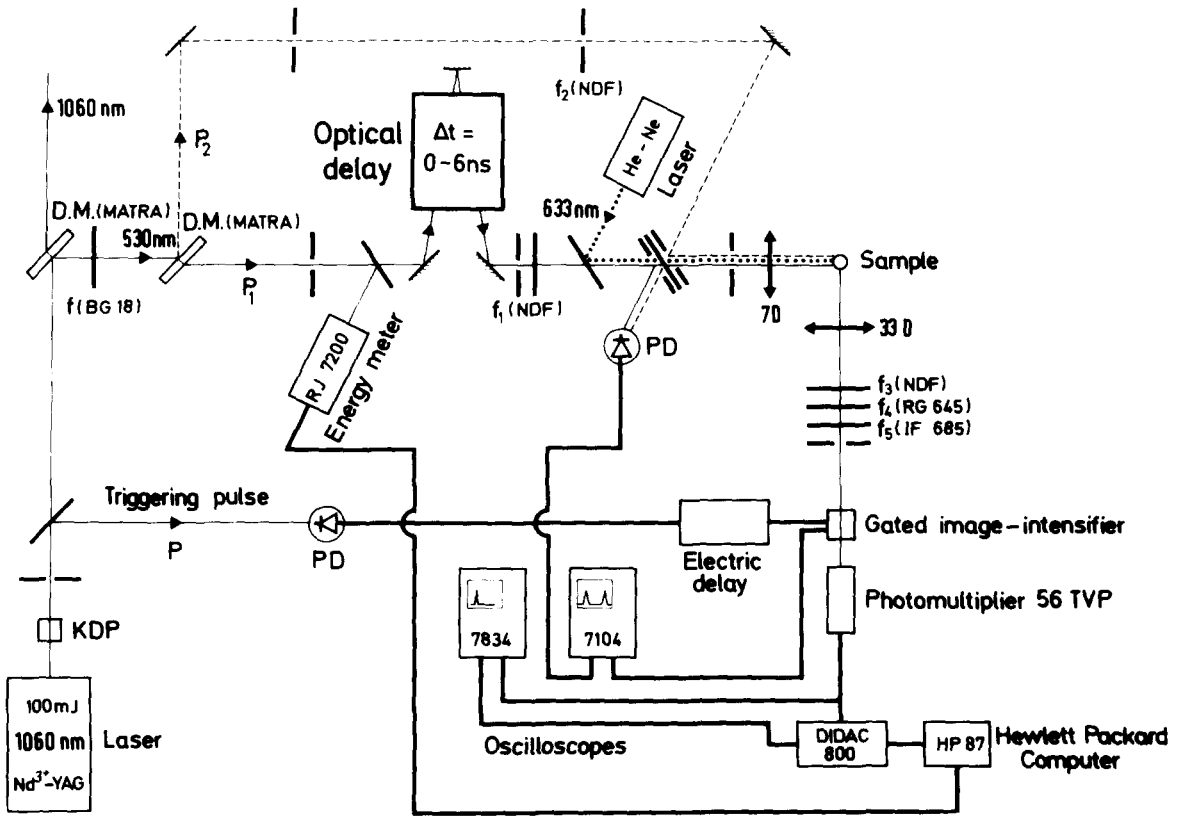

Fig. 2. Schematic diagram of the experimental apparatus. D.M., dichroic mirror (Matra); NDF, neutral density filter; BG 18 and RG 645, colored glass filters (Schott); IF 685, 685 nm interference filter; 7834 and 7104, oscilloscopes (Tektronix); PD, fast photodiode; KDP, KH_2PO_4 doubling crystal; DIDAC 800, multichannel analyzer (Intertechnique).

rors and beam splitters was utilized to render P_1 colinear with P_2 and with a light beam of a 5 mW He-Ne laser, and to direct these beams onto a $6 \cdot 10^{-3}$ cm^2 area spot on the sample. A set of calibrated neutral density filters (f_1, f_2) were utilized to vary the intensities of the pulses P_1 and P_2, and to adjust the intensities so that they were within 10% of one another.

The chloroplast suspensions were chilled in an ice-bath and circulated through a 1 mm diameter glass capillary tube, a portion of which was exposed to the laser beam(s) [4]. The fluorescence emitted by the chloroplasts was focussed onto the entrance diaphragm of the image intensifier protected by neutral density filters (f_3), a Schott RG645 cut-off filter (f_4) and a 685 nm narrow-band (half-width at half-maximum 10 nm) interference filter (f_5). The image intensifier was gated on for intervals of 20 ns, thus allowing for the detection of the fluorescence generated by both pulses independent of the delay time Δt. The intensified light signals were detected by an Amperex 56TVP photomultiplier tube which was positioned behind the image intensifier. The intensity of each pulse, or of each pair of pulses, was monitored by an energy meter (RJ 7200, Laser Precision Corp.). The signals from the photomultiplier tube and the pulse energy meter were entered into a DIDAC 800 (Intertechnique) multichannel analyzer and the results of 100 successive experiments were averaged utilizing either P_1 or P_2 alone, or a combination $P_1 + P_2$ of the pulses. A Hewlett-Packard 87 computer linked to the DIDAC was utilized to calculate the corresponding values of the fluorescence yields F_1, F_2, F_{1+2}, and the changes in the yield ΔF.

The Tektronix oscilloscopes 7104 and 7834 allowed for additional or independent monitoring of

the photomultiplier and amplifier outputs, as well as the detection of the reference signal pulse from the fast photodiode and from the image intensifier.

Results

Single pulse experiments

A fluorescence quenching curve obtained with dark-adapted chloroplasts, i.e., with open reaction centers, displaying typical error bars, is shown in Fig. 3. The experimental points represent averages obtained from nine different chloroplast samples; for each sample the averages are calculated on the basis of six different measurements, which in turn constitute the results of 100 laser pulses as described above; the error bars shown in this figure are characteristic of data obtained for one given chloroplast sample. The solid line drawn through the data represents the smoothest fit to the experimental averages. This F_1 curve is normalized to unity at a laser pulse intensity of $6 \cdot 10^{12}$ photons per cm^2. Considering each of the individual curves obtained for the nine different samples (data not shown), it is clear that there is a rise in the fluorescence yield at lower pulse energies, and a decrease in the yield for energies above approx. $1 \cdot 10^{13}$ photons per cm^2, thus confirming the earlier data [4,7].

If the saturating He-Ne laser beam is superimposed on the sample during the experiments, the rise in the fluorescence yield is not observed. The decline in the yield with increasing laser-pulse intensity sets in within the range of 10^{12} to 10^{13} photons per cm^2 [4].

Double-pulse experiments ($\Delta t = 0$)

The F_1 curve shown in Fig. 3 can be utilized to calculate a ΔF curve. In such a derivation it is supposed that the two hypothetical pulses overlap exactly in time and space ($\Delta t = 0$) and have the same energy. Thus, the single pulse fluorescence yield curve in Fig. 3 is used to read off pairs of fluorescence yield values $F_1(I)$ and F_{1+2} $(2I)$, where ΔF is calculated according to Eqn. 1. The result of such a calculation is shown in Fig. 4 (solid line). The experimental data were obtained utilizing pairs of picosecond pulses of equal intensities (within 10%) and Δt adjusted to zero as described in the Experimental Procedure section. It is important to point out that the error bars in the double-pulse experiments (Fig. 4) are smaller than those in the single-pulse experiments (Fig. 3). This is due to the fact that F_1 and F_{1+2} are measured at the same pulse intensities I utilizing a single set of attenuation filters; furthermore, the measurements are made within a small time-interval so that errors due to the evolution of the fluorescence characteristics of the sample and the laser beam are minimized. On the other hand in the single pulse experiments of Fig. 3, the excita-

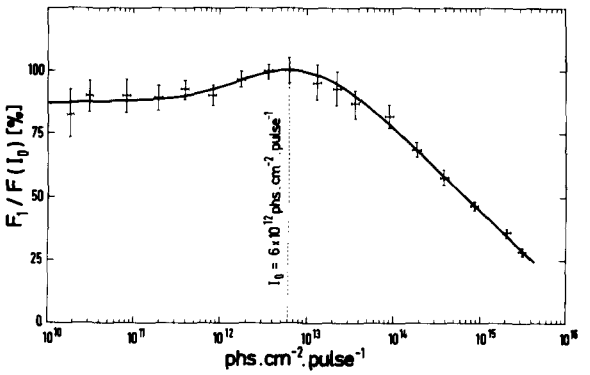

Fig. 3. Fluorescence quenching curve (fluorescence signal divided by the incident laser intensity) measured with dark-adapted chloroplasts; single- or double-pulse excitation with $\Delta t = 0$ (overlap of the two pulses in time and space) give the same results after adjustment to the same excitation intensity on the horizontal scale.

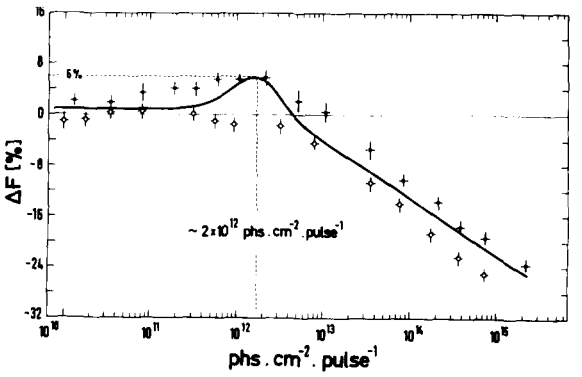

Fig. 4. Fluorescence yield change (ΔF) curve (solid line) as a function of laser pulse intensity calculated from the data of the fluorescence quenching curve shown in Fig. 3. The experimental data are represented as (●) for dark-adapted chloroplasts and as (○) for light-adapted chloroplasts (background illumination by He-Ne laser). In this case a positive rise in ΔF is not observed (see text).

tion intensities are varied by changing the attenuation filters; in addition, there are small changes in the sample characteristics and the laser beam, thus introducing errors when the measurements are repeated at different intensities involving an interchange of the set of attenuation filters and time-intervals of up to 2 h.

With dark-adapted chloroplasts, the data should ideally overlap with the hypothetical solid line in Fig. 4; the actually observed deviations of the data from the hypothetical curve are attributed to inhomogeneities in the pulse intensities and imperfections in the spatial overlap of these pulses and overlap in the time domain. However, qualitatively, the data reproduce the general shape of the hypothetical curve, since $\Delta F > 0$ when $I < 10^{13}$ and $\Delta F < 0$ when $I > 10^{13}$ photons per cm^2 per pulse.

In the case of closed reaction centers, i.e., upon background illumination with the He-Ne laser, the rise in ΔF in the lower intensity regime is not observed. The ΔF curve is equal to zero at the lower intensity values and assumes increasingly negative values as the energies of the pulse pairs are increased.

Double-pulse experiments ($\Delta t > 0$)

The ΔF curves depend on the delay time Δt between the two pulses. For simplicity of presentation, only the smoothed lines drawn through the actual data points are shown in Fig. 5 for dark-adapted chloroplasts, and in Fig. 6 for chloroplasts exposed to He-Ne laser background illumination. The error bars are omitted in these representations, but their magnitudes are the same as those depicted for the $\Delta t = 0$ case in Fig. 4.

Referring to the case of open reaction centers (Fig. 5), it was observed that for $\Delta t = 1$ ns, ΔF is only slightly positive for pulse energies below approx. 10^{13} photons per cm^2, and is zero for the whole range of pulse intensities for $\Delta t = 3$ and 6 ns. For these latter two time-intervals it is evident that the effects produced on the fluorescence yield by the two pulses are completely decorrelated, i.e., there is no effect of the pulse P_1 on the fluorescence yield generated by pulse P_2. However, for shorter Δt values a pronounced variation in ΔF is observed. The $\Delta t = 0$ case is discussed above. Near pulse energies of 10^{12} photons per cm^2, an increasingly positive ΔF is observed for $\Delta t = 0$, 25 and 50 ps, and then ΔF decreases reaching eventually a value of zero as Δt is increased above 150 ps. Above approx. $2 \cdot 10^{12}$ photons per cm^2 a decline in ΔF sets in for all Δt values. At higher energies (over 10^{14} photons per cm^2) the magnitude of the negative ΔF values decreases smoothly with increasing Δt.

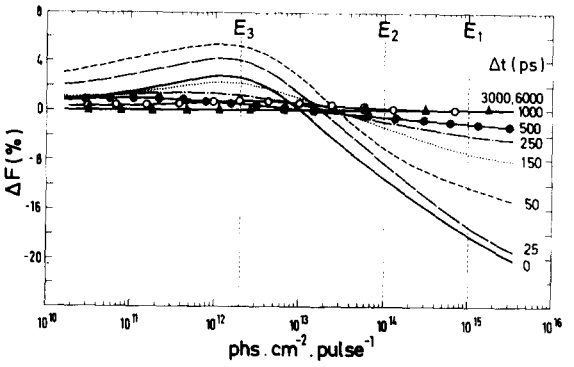

Fig. 5. Dependence of the fluorescence yield change ΔF on pulse intensities for different delay times Δt (ps) between the pulses P_1 and P_2 for dark-adapted chloroplasts. The typical erorr bars (not shown) are the same as those depicted for open reaction centers in Fig. 4. ●———●, 500 ps; ○———○, 1000 ps; ▲———▲, 3000 or 6000 ps (the data are identical for these two delay times); the shorter delay times are marked on the figure.

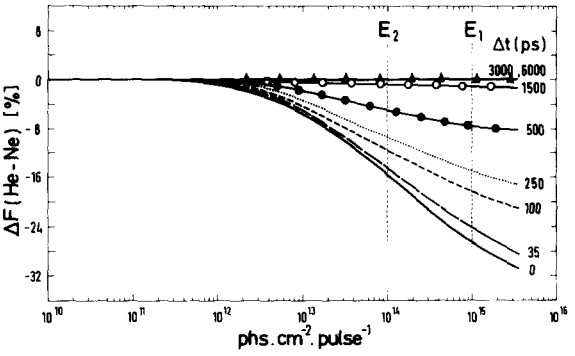

Fig. 6. Dependence of the fluorescence yield change ΔF on the delay time Δt (ps) between the pulses P_1 and P_2 for chloroplasts exposed to the saturating He-Ne laser background illumination. The error bars (not shown) are the same as those depicted for the $\Delta t = 0$ case for closed reaction centers in Fig. 4. ▲———▲, 3000 or 6000 ps (the data are the same for these two delay times); ○———○, 1500 ps; ●———●, 500 ps; the shorter delay times are marked directly on the figure.

In the case of closed reaction centers, only zero and negative values of ΔF are observed (Fig. 6) and the two pulses appear to be completely decorrelated for $\Delta t \gtrsim 1.5$ ns. The observation of positive values of ΔF at low energies in the case of dark-adapted chloroplasts (Fig. 5) can thus be attributed to effects arising from variations in the states of the reaction centers on short time-scales.

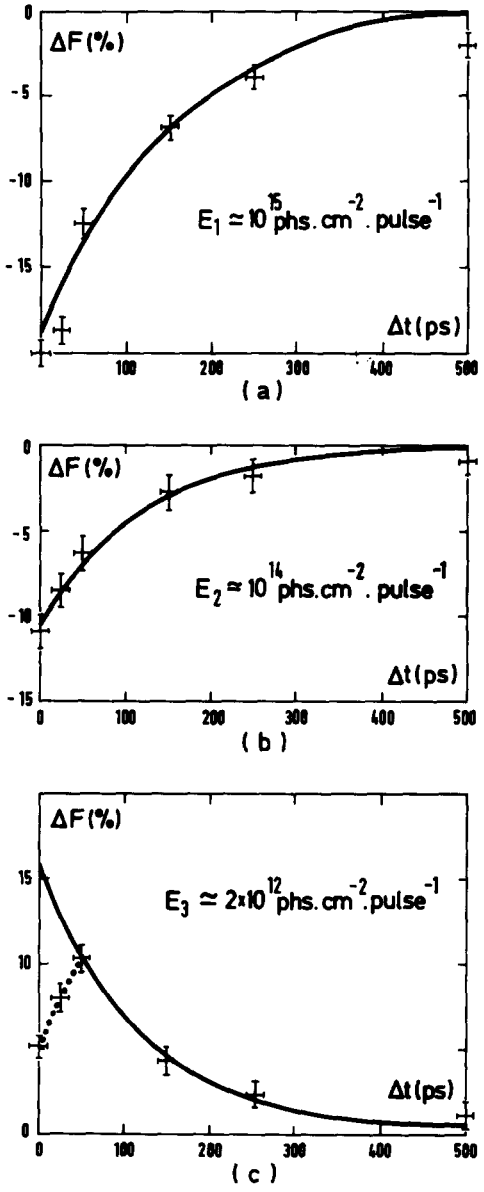

Fig. 7. Amplitude of the fluorescence yield change ΔF as a function of the delay time (ps) between the pulses P_1 and P_2 for dark-adapted chloroplasts at the three fixed energies indicated in Fig. 5. (a) $E_1 = 1 \cdot 10^{15}$ photons per cm^2 per pulse; (b) $E_2 = 1 \cdot 10^{14}$ photons per cm^2 per pulse; (c) $E_3 = 2 \cdot 10^{12}$ photons per cm^2 per pulse. Note that for $\Delta t < 50$ ps the amplitude ΔF exhibits a rise (for details see text). The solid lines represent plots of the exponential function of $\Delta F = \Delta F(0) e^{-\Delta t/\tau}$ with the constants indicated in Table I.

Time-dependence of ΔF at fixed excitation intensities

The negative values of ΔF at high pulse energies are indicative of fluorescence quenching due to singlet-singlet exciton annihilation, and reflect the effects of excitons created by the first pulse on the fluorescence generated by the second pulse. Thus a decrease in the magnitude of ΔF at the

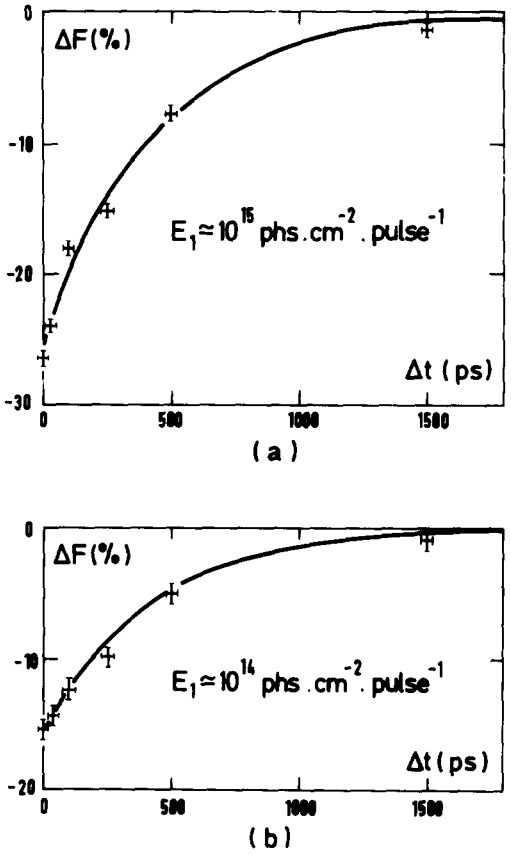

Fig. 8. Amplitude of the fluorescence yield change ΔF as a function of the delay time Δt (ps) between the pulses P_1 and P_2 for light-adapted chloroplasts (exposed to saturating He-Ne laser background illumination) at the two fixed energies indicated in Fig. 6. (a) $E_1 = 1 \cdot 10^{15}$ photons per cm^2 per pulse; (b) $E_2 = 1 \cdot 10^{14}$ photons per cm^2 per pulse. The solid lines represent plots of the exponential function $\Delta F = \Delta F(0) e^{-\Delta t/\tau}$ with the constants shown in Table I.

TABLE I

CHARACTERISTICS OF THE DIFFERENTIAL FLUORESCENCE PARAMETER $\Delta F(\Delta t) = \Delta F(0)e^{-\Delta t/\tau}$

This parameter describes the yield enhancement ($\Delta F > 0$), or quenching effect ($\Delta F < 0$), due to excitons produced by the first pulse on the fluorescence yield of the second pulse incident on the sample after a time interval Δt. The three energies (Figs. 5 and 6) are $E_1 = 10^{15}$, $E_2 = 10^{14}$ and $E_3 = 2 \cdot 10^{12}$ photons per cm^2 per pulse. Note: the spread in the τ values (obtained from individual experiments such as in Figs. 7 and 8) are smaller than reported in this table; these values are averages based on experiments performed with nine different samples.

	E_1		E_2		E_3	
	$\Delta F(0)$ (%)	τ(ps)	$\Delta F(0)$ (%)	τ(ps)	$\Delta F(0)$ (%)	τ(ps)
Open reaction centers	-19 ± 3	150 ± 50	-11 ± 2	120 ± 50	16 ± 4 *	120 ± 50 *
Closed reaction centers	-26 ± 3	400 ± 100	-16 ± 2	400 ± 100		

* For $\Delta t > 50$ ps.

high pulse energies with increasing Δt should, in principle, be correlated with the lifetime of these singlet exciton quenchers. In fig. 7a and b the values of ΔF are plotted as a function of Δt at two fixed energies of 10^{14} and 10^{15} photons per cm^2 per pulse. The solid lines represent plots of the exponential function:

$$\Delta F = \Delta F(0)e^{-\Delta t/\tau} \quad (3)$$

where τ is a constant related to the lifetime of the excitons. The values of $\Delta F(0)$ reflect the magnitudes of ΔF for complete overlap of the pulses ($\Delta t = 0$). At low pulse energies ($I = 2 \cdot 10^{12}$ photons per cm^2 per pulse), the Δt dependence of ΔF is depicted in Fig. 7c, showing both the rise of ΔF for small intervals, and the decline at large intervals fitted by Eqn. 3. The values of $\Delta F(0)$ and τ for each one of these plots are summarized in Table I. The values of τ lie in the range of 140 ± 60 ps. Most of the rise of ΔF observed for $\Delta t < 50$ ps occurs on time-scales in which there are still varying degrees of overlap between the two pulses in the time-domain. In view of this fact and the few experimental points, a quantitative estimation of the risetime is not justified.

For closed reaction centers, the Δt dependence of ΔF is also well represented by the exponential function (Fig. 8a and b).

Identical values of $\tau = 400$ ps are obtained at the fixed pulse intensities of 10^{14} and 10^{15} photons per cm^2.

Discussion

Increases in the fluorescence yield with increasing excitation intensity are generally attributed to changes in the state of the PS II reaction centers. Decreases in F with increasing laser pulse intensities on the other hand, have been explained in terms of bimolecular exciton annihilation.

It has been usually assumed for single picosecond pulse excitation that both singlet excitons are mobile and that the rate of disappearance of excitons is proportional to γn^2, where γ is the bimolecular annihilation coefficient and n is the density of mobile singlet excitons [7,9,16–19]. Since the fluorescence of chloroplasts is heterogeneous in nature, possibly originating from different pigment systems even at room temperature, the previous picture of singlet-singlet exciton annihilation occurring between two mobile excitons in a homogenous antenna pigment bed may not be applicable [9,10]. However, other mechanisms are possible such as annihilation in smaller pigment pools (i.e., the chlorophyll *a* antenna molecules closely associated with PS II reaction centers), or annihilation of a trapped excitation in such pigment pools by excitons arriving from the light-harvesting pigment bed. Evidence for such annihilation mechanisms in smaller pigment pools in chloroplasts at low temperature is described elsewhere [20].

At very high picosecond-pulse excitation intensities the average distance between excitations in the membranes may be sufficiently small, so that

energy transfer and quenching may occur by the Förster mechanism. However, under the conditions of our experiments (10^{15} photons per cm^2 per pulse) this mechanism is unlikely; utilizing the absorption crossection $\sigma_{530} = 1.6 \cdot 10^{-17}$ cm^{-2} it can be calculated [17] that only one out of 60 chlorophyll molecules are initially excited at the highest pulse energy used in this work. Utilizing an average value of 2.4 nm^2 per chlorophyll molecule in membranes of green plants [21], the average initial distance between excited molecules is about 1.3 nm. Since this value is about twice as large as the typical Förster transfer radius [22], singlet-singlet exciton annihilation before exciton motion has occurred is not expected to be an important mechanism in fluorescence quenching.

Exciton-exciton annihilation

Up till now, the evidence for exciton-exciton annihilation was: (i) intensity-dependent lowering of the fluorescence yield as, for example, shown in Fig. 3, and (ii) a lowering of the mean fluorescence decay time with increasing pulse intensity [19]. Our double-pulse experiments in which ΔF is measured as a function of the delay time between the two pulses constitute additional proof for this phenomenon, since the excitations generated by the first pulse are shown to decrease the fluorescence yield of the second pulse. According to Figs. 4 and 6, it appears that annihilation sets in at pulse intensities in the range of $(1-2) \cdot 10^{12}$ photons per cm^2, which is a lower threshold than was previously reported.

Heterogeneity of fluorescence decay components and exciton annihilation

Three fluorescence decay phases termed the fast (90–130 ps), the intermediate or middle (300–600 ps), and the long (1.4–2.3 ns) components have been characterized [12–15]. The relative amplitudes of these three components are 15–30%, over 70%, and 3–15%, respectively in the F_0 state. In the F_{max} state the amplitude of the slow component increases dramatically, while that of the fast component diminishes [13].

The long component is attributed to the Klimov mechanism which involves the generation of luminescence by charge recombination in closed reaction centers [23]. The origins of the first two fluorescence components are not clear. It has been speculated [13] that the fast component is due to the transfer of excitons from either PS I antenna, or PS II antenna molecules near the traps, to the PS I and PS II reaction centers, respectively. The intermediate component has been tentatively attributed to energy migration from the Chl *a/b* light-harvesting protein complexes which are more distant from the PS II traps [12,13]. Alternatively, it has been suggested by one of us [24] that the short component arises from charge recombination within open PS II reaction centers; in this latter mechanism the initial trapping of the excitation energy, which essentially originates from the light-harvesting protein complexes, would be extremely rapid.

An important point to note is that measurements of fluorescence decay profiles (or yields) are incapable of distinguishing between the emission components arising from trapped excitons, mobile excitons within the light-harvesting antenna pigments, or excitons localized in smaller pigment pools. These different types of exciton populations, while actively contributing to the overall fluorescence yields, are not expected to contribute equally to exciton annihilation phenomena. Mobile excitons may manifest themselves as quenchers in double pulse experiments as long as the separation Δt between the two pulses is comparable to the decay kinetics of these excitons.

Kinetics of decorrelation of the fluorescence quenching

In open reaction centers the fluorescence signals generated by the two pulses appear to become completely decorrelated from one another within approx. 300 ps. The 140 ± 60 ps decorrelation time-constant is comparable to that of the fast decay component observed in the single photon counting experiments [12–15]. Values of ΔF smaller than 2–3% cannot be excluded for $\Delta t \gtrsim 300$ ps; nevertheless, it appears that the other two fluorescence decay components do not manifest themselves as exciton quenchers, even though the intermediate and long components contribute more than one half of the overall fluorescence. The characteristic time of decorrelation between the two pulses, measured at the two different pulse energies of 10^{14} and 10^{15} photons per cm^2, is the

same within experimental error (Fig. 7a and b). This indicates that the rate of decay of the fast phase exhibits at best a weak dependence on the pulse intensity [25].

In closed reaction centers the two pulses remain correlated up to approx. 1.5 ns, and the characteristic decorrelation time is 400 ± 100 ps (Table I). Furthermore, the fast decorrelation time of 140 ± 60 ps observed in the F_0 state is not apparent in the F_{max} state. It is interesting to note that the long-lived excitons (approx. 2 ns) which give rise to the major proportion of the fluorescence yield when the centers are closed, are not efficient quenchers in exciton-exciton annihilation phenomena. The decay kinetics of the 400 ps component do not seem to depend on the energy of the pulses. The observation that the decorrelation times are insensitive to the energy oft he excitation pulses in intensity regimes in which exciton-exciton annihilation takes place, suggests a model in which the annihilations take place in the core antenna molecules surrounding the PS II reaction centers, rather than in the light-harvesting antenna pigment bed. Two mutually nonexclusive models can be proposed to rationalize our observations.

In the first model, the excitons migrate in the light-harvesting pigment bed and decay by trapping by the reaction centers (generation of P*-680) with a characteristic lifetime of 140 ± 60 ps. The observation of a 400 ± 100 ps decorrelation time in closed reaction centers can then be rationalized by the well-known mechanism [2] in which the exciton lifetime is increased when the PS II reaction centers are converted from the quenching state P-680-I-Q (P-680 is the primary donor, I the intermediate acceptor, Q the first quinone acceptor) to a less efficient quenching state P-680-I-Q^-. A uniform lengthening of the exciton lifetime, together with the apparent disappearances of the fast phase upon closure of the reaction centers, implies that the exciton is reinjected into the antenna pigment bed.

In the second model, the excitons created in the light-harvesting pigment bed migrate very rapidly (significantly faster than approx. 140 ps) towards the PS II core antenna, where they generate a new state of the reaction center (and/or core antenna), which in turn acts as a quencher of excitons generated by the second pulse. In open reaction centers it is assumed that the characteristic decorrelation time of 140 ± 60 ps corresponds to the decay of this state, which may be due to the time required for the stabilization of the charge on the quinone acceptor according to the reaction:

$$P^*\text{-}680\text{-}I\text{-}Q \rightarrow P^+\text{-}680\text{-}I^-\text{-}Q \rightarrow P^+\text{-}680\text{-}I\text{-}Q^-$$

as proposed in Ref. 24. In this case the 400 ± 100 ps decorrelation time observed in the case of closed reaction centers could be ascribed to the decay time of the special pair in the state P^+-680-I^--Q^- (back reaction, conversion to triplets).

The absence of the slow fluorescence component in the case of closed reaction centers can be understood in terms of the difference in the state of the system, following excitation, in the two experiments. The low-intensity picosecond experiments [12] probe the decay profiles of excitons when almost all of the reaction centers are in the state P-680-I-Q^- and when there are few excitations per reaction center, while in our double-pulse experiments the second pulse probes the lifetimes of many interacting excitons after all of the reaction centers have been synchronously converted to the state P^+-680-I^--Q^- by the first pulse.

The fluorescence induction at $\Delta t < 50$ ps

In the case of open reaction centers an increase in the fluorescence yield with increasing pulse separation appears up to about $\Delta t \approx 50$ ps, and as long as the pulse energy does not exceed approx. $1 \cdot 10^{13}$ photons per cm^2. These positive ΔF values thus indicate that the first pulse has an enhancement effect on the fluorescence yield of the second pulse, which is quite different from the negative effect observed at higher excitation energies for which $\Delta F < 0$. The positive ΔF values observed in Fig. 7c for excitation energies of approx. $2 \cdot 10^{12}$ photons per cm^2 appear to be related to the enhancement in the yield observed at low excitation energies in the single pulse excitation case (Fig. 3 and Refs. 4 and 7).

It is clear that the enhancement of the yield at low pulse energies is related to the existence of open reaction centers, since the enhancement is not observed when the reaction centers are closed by He-Ne laser background illumination (Figs. 4 and 6). However, because of the short time-scales,

this phenomenon is different from the normal fluorescence induction which is characterized by a time constant of 28 ± 4 ns [4]. It is possible that the fast approx. 50 ps risetime represents the migration time of excitons from the light-harvesting pigment bed and the trapping by the PS II reaction centers (generation of P*-680) as described above in the context of the second model. If this hypothesis is correct, then the complex behavior of ΔF shown in Fig. 7c for low energies would be due to a generation (ΔF increase) and the decay (ΔF decrease) of the P^+-680-I^--Q state.

It is interesting to note that the low-intensity fluorescence yield enhancement observed by us and by Hirsch et al. [7] using picosecond pulses, has also been noted by Haehnel et al. [13] who also used single picosecond pulse excitation (approx. 10 ps duration) and the single photon counting method. While increasing the pulses intensity above $2 \cdot 10^{10}$ photons per cm^2 by a factor of approx. 20 (630 nm excitation), they observed that the yield of the second component increased by approx. 80%, while the yield of the first component remained constant; the corresponding decay times τ_1 and τ_2 also remained constant in the same intensity regime.

There is another puzzling aspect of this enhancement behavior which should be noted. The fluorescence yield rise effect is clearly linked to the reaction centers, and yet the excitation pulse intensity range of 10^{10}–10^{13} photons per cm^2 is lower than expected from a knowledge of the effective absorption crossections per reaction center of about 10^{14} photons per cm^2 [4,26,27]. The low-intensity fluorescence induction effects discussed here occur at intensities which are below this value by factors of 10–1000. The only possible explanation which can be advanced at this time is that there is a heterogeneity of reaction-center-associated light-harvesting antenna complexes [28], some having much higher absorption crosssections than others.

Conclusions

The double-pulse technique described in this work can be utilized to provide new information on fluorescence phenomena in chloroplasts on subnanosecond time-scales. While standard fluorescence yield experiments and decay profile determinations cannot distinguish between the possible different origins of the fluorescence emissions, the double-pulse method can, in principle, provide information on densities of mobile exciton populations in photosynthetic membranes. Furthermore, the double-pulse technique can be utilized to probe the time dependence of the changes in the fluorescence-quenching properties of the system after the conversion of all of the reaction centers to the state P^+-680-I^--Q or P-680$^+$-I^--Q^-. This represents a different state of the system as compared to the one encountered in the single-photon counting experiments where, due to the low level of excitation, the instantaneous concentrations of these states are always very low. The characteristic decorrelation time between the fluorescence quenching properties of the two pulses is relatively insensitive to the energy of the first excitation pulse, but is clearly dependent on the state of the reaction center. The time scales of 140 ± 60 and 400 ± 100 ps observed for the decorrelation between the two pulses for dark-adapted and light-adapted chloroplasts, respectively, most probably reflect very primary events (exciton trapping, initial charge separation and/or recombination) taking place in the PS II reaction centers.

Acknowledgements

This work was in part supported by the National Science Foundation, Grant PCM 83-08190, to N.E.G.

References

1 Lavorel, J. and Etienne, A.L. (1977) in Primary Processes of Photosynthesis (Barber, J., ed.), pp. 203–268, Elsevier, Amsterdam
2 Murata, N., Nishimura, M. and Takamiya, A. (1966) Biochim. Biophys. Acta 120, 23–33
3 Mauzerall, D. (1972) Proc. Natl. Acad. Sci. USA 69, 1358–1362
4 Deprez, J., Dobek, A., Geacintov, N.E., Paillotin, G. and Breton, J. (1983) Biochim. Biophys. Acta 725, 444–454
5 Mauzerall, D. and Malley, M. (1971) Photochem. Photobiol. 14, 225–227
6 Butler, W.L. (1972) Proc. Natl. Acad. Sci. USA 69, 3470–4322
7 Hirsh, I., Neef, E. and Fink, F. (1982) Biochim. Biophys. Acta 681, 15–20

8 Campillo, A.J., Shapiro, S.L., Kollman, V.H., Winn, K.R. and Hyer, R.C. (1976) Biophys. J. 16, 93–97
9 Geacintov, N.E., Breton, J., Swenberg, C.E. and Paillotin, G. (1977) Photochem. Photobiol. 26, 629–638
10 Breton, J. and Geacintov, N.E. (1980) Biochim. Biophys. Acta 594, 1–32
11 Sonneveld, A., Rademaker, H. and Duysens, L.N.M. (1979) Biochim. Biophys. Acta 548, 536–551
12 Haehnel, W., Nairn, J.A., Reisberg, P. and Sauer, K. (1982) Biochim. Biophys. Acta 680, 161–173
13 Haehnel, W., Holzwarth, A.R. and Wendler, J. (1983) Photochem. Photobiol. 37, 435–443
14 Karukstis, K.K. and Sauer, K. (1983) Biochim. Biophys. Acta 722, 364–371
15 Gulotty, R.J., Fleming, G.R. and Alberte, R.S. (1982) Biochim. Biophys. Acta 682, 322–331
16 Paillotin, G., Swenberg, C.E., Breton, J. and Geacintov, N.E. (1979) Biophys. J. 25, 513–533
17 Geacintov, N.E. and Breton, J. (1982) in Biological Events Probed by Ultrafast Laser Spectroscopy (Alfano, R.R., ed.), pp. 157–191, Academic Press, New York
18 Swenberg, C.E., Geacintov, N.E. and Pope, M. (1976) Biophys. J. 16, 1447–1452
19 Campillo, A.J., Kollman, V.H. and Shapiro, S.L. (1976) Science 193, 227–229
20 Wittmershaus, B.P., Nordlund, T.M., Knox, W.H., Knox, R.S., Geacintov, N.E., and Breton, J. (1985) Biochim. Biophys. Acta 806, 93–106
21 Colbow, K. and Danyluk, R.P. (1976) Biochim. Biophys. Acta 440, 107–121
22 Knox, R.S. (1976) in Bioenergeties of Photosynthesis (Govindjee, ed.), pp. 183–221, Academic Press, New York
23 Klimov, V.V., Klevanik, A.V., Shuvalov, V.A. and Krasnovsky, A.A. (1977) FEBS Lett. 82, 183–186
24 Breton, J. (1983) FEBS Lett. 159, 1–5
25 Geacintov, N.E., Paillotin, G., Deprez, J., Dobek, A. and Breton, J. (1984) in Advances in Photosynthesis Research (Sybesma, C., ed.), Vol. I, pp. 37–40, Martinus Nijhoff/Dr. W. Junk Publishers, The Hague
26 Mauzerall, D. (1976) J. Phys. Chem. 80, 2301–2309
27 Ley, A.C. and Mauzerall, D. (1982) Biochim. Biophys. Acta 680, 95–106
28 Melis, A. and Homann, P.H. (1978) Arch. Biochem. Biophys. 190, 523–530